Entomological Science (2016) **19**, 188–200 doi: 10.1111/ens.12180

ORIGINAL ARTICLE

β-Ionone as putative semiochemical suggested by ligand binding on an odorant-binding protein of *Hylamorpha elegans* and electroantennographic recordings

Herbert VENTHUR[1,2], Jing-Jiang ZHOU[3], Ana MUTIS[2], Ricardo CEBALLOS[4], Rodrigo MELLA-HERRERA[5], Giovanni LARAMA[6], Andrés AVILA[6], Patricio ITURRIAGA-VÁSQUEZ[7], Manuel FAUNDEZ-PARRAGUEZ[7], Marysol ALVEAR[8] and Andrés QUIROZ[2]

[1] *Programa de Doctorado en Ciencias de Recursos Naturales, Universidad de La Frontera, Temuco, Chile,* [2] *Laboratorio de Química Ecológica, Departamento de Ciencias Químicas y Recursos Naturales, Universidad de La Frontera, Temuco, Chile;* [3] *Department of Biological Chemistry and Crop Protection, Rothamsted Research, Harpenden, Herts, UK;* [4] *Laboratorio de Ecología Química, Centro Tecnológico de Control Biológico, Instituto de Investigaciones Agropecuarias (INIA)-Quilamapu, Chillán, Chile,* [5] *Center of Waste Management and Bioenergy, Scientific and Technological Bioresource Nucleus, Universidad de La Frontera, Temuco, Chile,* [6] *Centro de Modelación y Computación Científica, Universidad de La Frontera, Temuco, Chile,* [7] *Laboratorio de Síntesis Orgánica, Departamento de Química, Facultad de Ciencias, Universidad de Chile, Las Palmeras, Santiago, Chile and* [8] *Departamento de Ciencias Químicas y Recursos Naturales, Universidad de La Frontera, Casilla 54-D, Temuco 4811230, Araucanía, Chile*

Abstract

Currently, odorant-binding proteins (OBPs) are considered the first filter for olfactory information for insects and constitute an interesting target for pest control. Thus, an OBP (HeleOBP) from the scarab beetle *Hylamorpha elegans* (Burmeister) was identified, and ligand-binding assays based on fluorescence and *in silico* approaches were performed, followed by a simulated binding assay. Fluorescence binding assays showed slight binding for most of the ligands tested, including host-plant volatiles. A high binding affinity was obtained for β-ionone, a scarab beetle-related compound. However, the binding of its analogue α-ionone was weaker, although it is still considered good. On the other hand, through a three-dimensional model of HeleOBP constructed by homology, molecular docking was carried out with 29 related ligands to the beetle. Results expressed as free binding energy and fit quality (FQ) indicated strong interactions of sesquiterpenes and terpenoids (α- and β-ionone) with HeleOBP as well as some aromatic compounds. Residues such as His102, Tyr105 and Tyr113 seemed to participate in the interactions previously mentioned. Both *in silico* scores supported the experimental affinity for the strongest ligands. Therefore, the activity of α-ionone, β-ionone and 2-phenyl acetaldehyde at antennal level was studied using electroantenography (EAG). Results showed that the three ligands are electrophysiologically active. However, an aliquot of β-ionone (represented by 3.0 ng) elicited stronger EAG responses in antennae of males than of females. Finally, the role of these ligands as potential semiochemicals for *H. elegans* is discussed.

Key words: Coleoptera, electroantennography, fluorescence binding assay, homology modeling, molecular docking, olfactory protein, Scarabaeidae.

INTRODUCTION

More than 30 years have passed since the first insect odorant-binding protein (OBP) was discovered (Vogt & Riddiford 1981). This OBP, identified in sensilla of the giant moth *Antheraea polyphemus* and named as pheromone-binding protein (PBP), is present mainly in

Correspondence: Andrés Quiroz, Universidad de La Frontera, Temuco, Casilla 54-D, Chile.
Email: andres.quiroz@ufrontera.cl
Jing-Jiang Zhou, Rothamsted Research, Harpenden, Herts. UK.
Email: jing-jiang.zhou@rothamsted.ac.uk

Received 22 May 2015; accepted 10 September 2015; first published 15 June 2016.

© 2016 The Entomological Society of Japan

males and it is proposed to bind pheromones. Although it is strongly suggested that insect OBPs transport odorants from olfactory pores of sensilla to olfactory receptors (ORs) (Kaissling 2013), other functions have been reported for insect OBPs: (i) ligand scavenging (Gong *et al.* 2009); (ii) ligand desorption (Kowcun *et al.* 2001); (iii) ligand recognition (Laughlin *et al.* 2008); and (iv) ligand protection (Ishida & Leal 2002). Nowadays, OBPs are divided in three subclasses, PBP, general odorant-binding protein (GOBP) and antennal-binding protein X (ABPx), for Lepidoptera. However, for Coleoptera, no difference has been made yet. It seems that scarab beetles can have a family of OBPs with two proteins (OBP1 and OBP2) and another family of conserved PBPs as the unique proteins present in antennae. However, very few studies on binding for scarab OBPs have been performed. Moreover, a limited number of these proteins have been identified in scarab beetles, considering that information from the only Coleopteran genome known to date, that of *Tribolium castaneum*, indicates the presence of up to 50 OBPs.

Considering the economic importance of scarab beetles during their larval stage (Leal 1998; Vuts *et al.* 2014), the binding characteristics of scarab beetle OBPs have been studied only recently. For instance, fluorescence binding assays have been performed on the *Holotrichia parallela* OBP1 (HparOBP1), which showed binding affinities to a wider range of volatiles such as β-ionone, hexyl benzoate and cinnamaldehyde (Ju *et al.* 2012). More recently, a putative cooperation among the *H. oblita* OBPs (HoblOBP1, HoblOBP2 and HoblOBP4) has been proposed. These OBPs may act as heterodimers, improving the binding affinity of ligands when the proteins are together (Wang *et al.* 2013). Later, Zhuang *et al.* (2014) reported the role of Tyr111 in the binding site of HoblOBP1 using molecular modeling approaches as well as experimental techniques to show how hexyl benzoate, β-ionone, cinnamaldehyde and myrcene cannot bind to the protein in the absence of Tyr111.

In Chile, *Hylamorpha elegans* is a characteristic beetle belonging to the subfamily Rutelinae, which is distributed from Region del Maule to Region de Los Lagos. This insect acquires a significant importance because of the damage caused to cereals and grass crops, where it feeds on roots during its larval stage. Likewise, the adult stage of *H. elegans* is characterized by feeding on leaves of trees such as *Nothofagus* species, especially *Nothofagus obliqua*. Less information is available around the adult stage of this scarab beetle and the odorants involved in its life cycle. Only two putative sex pheromones, 1,4-hydroquinone and 1,4-benzoquinone, have been reported (Quiroz *et al.* 2007). Likewise, a synergistic effect was proposed when 1,4-benzoquinone plus essential oil from *N. obliqua* significantly attracted males of the scarab beetle to traps baited with this blend. Hence, compounds from *N. obliqua* seem to be important in the behavior of *H. elegans*. An outstanding mating behavior driven by host-plant volatiles has been suggested to play an important role for scarab beetles in several studies (Ruther *et al.* 2000; Reinecke *et al.* 2002; Quiroz *et al.* 2007). Males are able to recognize females while they are eating using a sexual kairomone, which is proposed to be released by the attacked plant. Field observations are consistent with this behavior in *H. elegans*. A recent study on morphology and distribution of sensilla suggests that males of *H. elegans* have more chemosensory sensilla than females because males are able to find and recognize females while they are feeding on leaves of *N. obliqua* (Mutis *et al.* 2014). Another special behavior has been highlighted for this beetle: after copulation females fly to crops such as red clover, *Trifolium pratense*, to deposit their fertilized eggs (Artigas 1994). It is worth mentioning that the importance of the beetle relies on the larval stage as a result of the mentioned behavior. It is thought that such behavior could be driven by volatile compounds emitted by crops.

In this study the binding characteristics of an OBP (HeleOBP) present in antennae of both male and female *H. elegans* were examined. Thus, host-plant volatiles, putative sex pheromones and semiochemicals reported for other scarab beetles were considered for binding. Here, we have performed fluorescence binding assays to evaluate the affinity of the ligands mentioned before. Likewise, homology modeling and subsequently molecular docking were applied for a binding simulation. Finally, three strong ligands were selected for electroantennography, which showed significant activity at certain concentrations.

MATERIALS AND METHODS

Selection of volatiles as ligands

Volatiles trapped by Porapak Q and solid-phase micro extraction (SPME) from *N. obliqua* leaves along with volatiles from adult *H. elegans* females and males were included (H. Venthur, unpublished results, 2013). Moreover, those volatiles were matched with previous reports where volatiles were identified from the same tree (Quiroz *et al.* 1999). Finally, volatiles reported as semiochemicals for other scarab beetles were selected from the Pherobase database (http://www.pherobase.com/).

Insects and protein analysis

Male and female adults of *H. elegans* were captured by light-trap at the Regional Research Center INIA-Carillanca in Vilcún, Araucanía, Chile. Beetles were

© 2016 The Entomological Society of Japan

captured during the seasonal flight period, from 11 November 2011 to 27 January 2012, according to Quiroz *et al.* (2007). Scarab beetles were recorded daily and taken to the laboratory for determining sex and used for both protein analysis and RNA extraction. Thus, the antennae and hindlegs were detached from both males and females anesthetized on ice. Protein analysis was carried out according to the methodology described by Ishida *et al.* (2002). After homogenizing in 10 mM Tris-HCl (pH 8.0), samples were centrifuged for 2 × 10 min intervals at 13 500 g and 4°C. The supernatant was concentrated by centrifugation under vacuum then analyzed by 15% native polyacrylamide gel (PAGE).

Cloning of cDNA and amplification by PCR

The cDNA was synthesized by a SMART RACE cDNA Amplification Kit (Clontech, Terra Bella Avenue Mountain view, CA, USA) from total RNA obtained from 50 antennae of *H. elegans* males and females using RNAlater (for RNA stabilization and protection) and the RNeasy Kit (Qiagen, Hilden, Germany). For cDNA cloning, degenerated primers for *Phyllopertha diversa* OBPs (PdivOBP_1 and PdivOBP_2) were used (Wojtasek *et al.* 1999; Table S1) in combination with poly T primer. Polymerase chain reaction (PCR) was carried out with PCR Master Mix 2X (Fermentas; Thermo, Lithuania, EU). Thus, 40 cycles of a stepwise amplification program were carried out with 95°C for 30 s, 42°C for 30 s and 72°C for 2 min. The PCR products were sent for sequencing (Macrogen, Seoul, Korea) and analyzed by Sequence Scanner Software v1.0, and comparisons of sequences were carried out with nucleotide and protein BLAST searches (http://blast.ncbi.nlm.nih.gov/). Once the best sequences were confirmed as belonging to OBPs, EMBOSS translation (http://www.ebi.ac.uk/Tools/st/) was used to obtain the amino acid sequence of the protein. Gene-specific primers (GSPs) were designed according to 3′ sequence of the protein and used to obtain 5′-RACE (Table S1). The quality of the first cDNA strand was tested by PCR using primers designed according to conserved regions of actine in insects: actine-1, 5′-AA(C/T)TGGGA (C/T)GA(C/T)ATGGA(A/G)AA-3′ and actine-2, 5′-GCCAT(C/T)TC(C/T)TG(C/T)TC(A/G)AA(A/G)TC-′3. Actine DNA was amplified by 45 cycles with 1 min for denaturation at 94°C, 2 min for annealing at 45°C and 3 min for amplification at 72°C. The PCR products were analyzed in 0.8% agarose gel.

Sub-cloning in pNIC28–Bsa4 vector

In order to obtain a construct for bacterial expression, a previously cloned OBP gene was used for ligase-independent cloning (LIC). This method is characterized by efficient cloning that does not require restriction enzymes (Aslanidis & de Jong 1990). LIC of PCR products has been improved over time to a high-throughput (HTP) cloning, reaching efficiencies greater than 80% (Alzari *et al.* 2006). BsaI restriction enzyme was used to digest pNIC28–Bsa4 vector for 2 h at 50°C. Digested vector was loaded on 1% agarose gel and purified. The linearized vector was treated with 0.5 μL of T4 DNA polymerase and 10 mM deoxyguanosinetriphosphate (dGTP) for 30 min at 22°C. T4 DNA polymerase was inactivated by incubation for 20 min at 75°C. On the other hand, the identified OBP from *H. elegans* (HeleOBP) was cloned into a pGEM-T easy cloning vector. PCR for the construct using primers with BsaI adapters (Table S1) was performed as follows: 94°C for 3 min, 35 cycles of 94°C for 30 s, 60°C for 30 s, 72°C for 1 min and extension at 72°C for 10 min. PCR product was cleaned and treated with T4 DNA polymerase and 10 mM deoxycytidinetriphosphate (dCTP) following the same conditions for pNIC28–Bsa4 vector. Both the treated vector and insert were mixed with 1:10 molar ratio in a total volume of 10 μL and incubated for 1 h at room temperature followed by transformation into BL21(DE3) competent cells. Correct gene insertions were tested by double digestion with both NdeI and SalI enzymes followed by sequencing.

Bacterial expression and purification

Positive colonies for the construct pNIC28–Bsa4–HeleOBP were used to inoculate 10 mL of fresh LB/kanamycin medium at 37°C. Protein expression was induced by adding isopropyl β-D-1-thiogalactopyranoside (IPTG) to 0.5 mM final concentration when the OD_{600} was 0.5–0.6. Cells were incubated for 3 h. To check the expression, aliquots of 200 μL of both induced and noninduced cells were used for SDS-PAGE analysis. Protein expression was scaled up with 500 mL of fresh LB/kanamycin medium in a 2 L Erlenmeyer flask and induced with IPTG 0.5 mM final concentration at 37°C overnight. Cells were collected and resuspended in 20 mM Tris-HCl (pH 7.4). Resuspended cells were lysed by sonication then centrifuged. After SDS-PAGE analysis of supernatant and pellet, recombinant HeleOBP (rHeleOBP) (present in inclusion body) was solubilized in 3.5 mL of 5 M urea, 2.5 mL of 10 mM DTT, 1 mL of 100 mM cystine and 15 mL of 5 mM cysteine. The sample was shaken at 4°C overnight. Dialysis of the protein sample was carried out against 20 mM Tris-HCl (pH 7.4). His-tagged HeleOBP was purified by two rounds of Ni ion affinity chromatography in an ÄKTA FPLC system (GE Healthcare, Hatfield, UK). Fractions were collected for each round and analyzed by SDS-PAGE. The pure protein was delipidated at pH 4.5 with 100 μL of Lipidex-1000

© 2016 The Entomological Society of Japan

(Perkin-Elmer, Massachusetts, USA) for 1 h on ice according to Siciliano *et al.* (2014). Refolding was carried out overnight by dialysis against 20 mM Tris-HCl (pH 7.4) at 4°C.

Fluorescence binding assays

Fluorescence measurements were performed in a luminescence spectrometer (LS50B; Perkin-Elmer) at 25°C with a 1 cm light path quartz cuvette and 5.0 nm slit for excitation and emission. Purified protein was diluted in 20 mM Tris-HCl (pH 7.4) to 2 μM concentration. Likewise, the fluorescent probe *N*-phenyl-1-naphthylamine (1-NPN) was dissolved in high-performance liquid chromatography (HPLC) purity grade methanol to 1 mM stock solution. To test the binding affinity of 1-NPN to HeleOBP, 2 μM solution of the protein was titrated with 1 mM of the probe with concentration from 2 to 24 μM. 1-NPN was excited at 337 nm, and the emission spectra were recorded from 380 to 440 nm. The affinities of 29 ligands were measured in competitive binding assays using 1-NPN as the fluorescent reporter and 4–40 μM concentrations for each competitor.

Binding data were collected and maximum fluorescence intensity values were plotted against free ligand concentrations. Bound ligand was determined from the values of fluorescence intensity assuming that the protein was 100% active with stoichiometry of 1:1 (ligand : protein) at saturation. Scatchard plots were used to linearize curves. Thus, IC_{50} values were used to calculate the dissociation constants for each ligand with the equation: $K_i = IC_{50}/(1 + [1\text{-NPN}]/K_{1\text{-NPN}})$, where [1-NPN] is the free concentration of 1–NPN and $K_{1\text{-NPN}}$ is the dissociation constant of the complex HeleOBP/1-NPN.

Multiple template-based homology modeling

The amino acid sequence of HeleOBP was submitted to the BLASTP program available on the NCBI website (http://www.ncbi.nlm.nih.gov/). Templates were selected based on the sequence identity (i.e. >30%) between crystal structures and HeleOBP. Multiple structure alignments were generated by the SALIGN command, which is implemented in MODELLER. Multiple templates were used to increase the accuracy of multiple structure alignment as reported by Sokkar *et al.* (2011). Two hundred models of HeleOBP were obtained using MODELLER9.10 (http://salilab.org/modeller). Best models were selected according to the discrete optimized protein energy (DOPE) score provided by the software. Likewise, best models were assessed using the theoretical validation package ProCheck (Laskowski *et al.* 1993). The modeled protein was visualized with PyMOL (http://www.pymol.org).

Molecular dynamics

Simulations were performed with NAMD v2.9 installed in the high-performance computer (HPC) Troquil Linux cluster at Centro de Modelación y Computación Científica (CMCC) at Universidad de La Frontera. CHARMM36 force field was used for all the simulations. The best modeled protein was solvated with water (TIP3P model) in a cubic box with a minimum distance of 5 Å (0.5 nm) between the protein and the edge of the box. The system net charge was neutralized by placing Na^+ or Cl^- randomly in the box. Likewise, the system was simulated under periodic boundary conditions with a cutoff radius of 12 Å (1.2 nm) for non-bonded interactions and a time step of 2×10^{-15} s. Alpha-carbon atoms (Cα) of secondary structures were fixed with a constant force of 1 kcal/mol/Å. A first energy minimization of 2000 steps was performed followed by heating through short simulations of 1×10^{-12} s at 50, 100, 150, 200, 250 and 300 K. Long simulations were kept at 300 K and 1 bar pressure in the NTP (referred to a constant number of particles, temperature and pressure) during 10 ns. The root-mean-square deviation (RMSD) trajectory tool was used to calculate the RMSD with reference to the starting structure. When the plotted RMSD did not show any large changes, coordinates were analyzed every 50 frames to obtain the best structure (lowest energy). The putative binding site and its volume were calculated by the CASTp server (http://sts-fw.bioengr.uic.edu/castp/calculation.php) (Dundas *et al.* 2006).

Molecular docking

Molecular docking was carried out three times for each ligand by AutoDock4.2 (Morris *et al.* 2009) using the refined structure of HeleOBP. Energy minimization for all chemical structures was performed by Chem3D software (http://www.cambridgesoft.com). Two hundred runs of Lamarckian genetic algorithm (GA) as the best method to find the lowest energy structures were used (Morris *et al.* 1998). Polar hydrogen atoms were added by the interface AutoDock Tools as well as establish torsional bonds. A grid box with 40 × 40 × 40 points and default space of 0.375 Å (0.0375 nm) was prepared by AutoGrid. The best binding modes were selected according to the lowest binding energy and the average of the three replicates was used to determine K_i according to $K_i = e^{\Delta G/RT}$. For the best conformations, two parameters for comparisons were selected: (i) free binding energy; and (ii) fit quality (FQ), which is an independent-size score for comparison of wider range of sizes in ligands. The ligand efficiency (LE) of a compound can be defined as the

© 2016 The Entomological Society of Japan

binding energy divided by its molecular size. To calculate FQ, the following equations $LE\_Scale = 0.0715 + (7.5328/HA) + (25.7079/HA^2) + (361.4722/HA^3)$ and $FQ = LE/LE\_Scale$ were used according to Bembenek *et al.* (2009). *LE_Scale* is the scaling of raw ligand efficiencies and *HA* is the number of heavy (non-hydrogen) atoms. Thus, compounds considered as good ligands are those with FQ near 1.0. On the contrary, lower FQ relates to poor ligand efficiencies (Reynolds *et al.* 2007; Bembenek *et al.* 2009). Therefore, to narrow the number of strong ligands according to the *in silico* approach we considered $FQ \geq 0.70$ as the cutoff.

Electroantennographic recordings

The antennal responses of adult females and males of *H. elegans* were determined by EAG according to the methodology described by Reinecke *et al.* (2005) with some modifications. Five antennae per sex were excised from the heads, where lamellae were carefully separated from the rest of antennal segments. Subsequently, a lateral lamella was excised in order to expose one side of the middle lamella, where olfactory sensilla are located (Mutis *et al.* 2014). Signals from antennae were conducted and recorded by Syntech equipment (Kirchzarten, Germany). Recorded data were displayed and analyzed by GcEad 2012 v1.2.4 software. An aliquot of 30 µL of α-ionone, β-ionone and 2-phenyl acetaldehyde in hexane (0.1, 1.0, 10, 100 and 1000 ppm, being 3.0, 30, 300, 3000 and 30 000 ng of stimulus, respectively) was loaded in a piece of filter paper (2 cm^2), which was then inserted into a glass Pasteur pipette. Each odor stimulus was delivered as a continuous airstream (500 mL/min) from the Pasteur pipette for 2.0 s. Intervals of 60 s between puffs were used to ensure antennal recovery.

Statistical analyses

To minimize any variation among antennae, EAG responses were corrected according to the solvent amplitude before and after the stimulus. This was carried out by the formula $R_c = R_s - ((R_{sb} + R_{sa})/2)$ (Guo & Li 2009), where R_c = corrected response, R_s = response to the stimulus, R_{sb} = response to the solvent before stimulus and R_{sa} = response to the solvent after stimulus. Thus, to determine differences of EAG responses to the concentrations used for each stimulus, data were submitted to analysis of variance ($P < 0.05$) and the Tukey test ($P < 0.05$) for group separation. Finally, the Student's *t*-test ($P < 0.05$) was used to evaluate differences in EAG response between *H. elegans* males and females.

RESULTS

Sequence analysis, sub-cloning and expression of HeleOBP

The cDNA obtained from antennae of *H. elegans* consisted of 348 bp with a high sequence identity of 95–98% with other PBPs and OBPs reported for scarab beetles. The gene was clustered with a large group of scarab beetle PBPs and named as HeleOBP as less information is available in terms of binding (Fig. S1). Thus, the *HeleOBP* gene was cloned from the antennae cDNA into a pGEM vector (Promega) with the aim of obtaining recombinant protein to perform binding assays. Ligase-independent cloning (LIC) was then performed to subclone the *HeleOBP* gene by PCR of pGEM–HeleOBP construct into an expression vector pNIC28 for the recombinant protein expression. The recombinant protein was expressed as inclusion bodies. Therefore, the protein was denatured with urea–DTT, re-natured using cysteine–cystine redox reaction and dialyzed to obtain a soluble form as reported by Plettner *et al.* (2000). However, the expressed OBP may contain endogenous ligands from the bacterial cells (Lagarde *et al.* 2011). Hence, delipidation was performed on purified protein (Siciliano *et al.* 2014). SDS-PAGE analysis of bacterial pellets and purified HeleOBP are shown in Figure 1 as homogenous recombinant protein. It is worth noting that a short His-tag section (22 amino acids) from the pNIC28

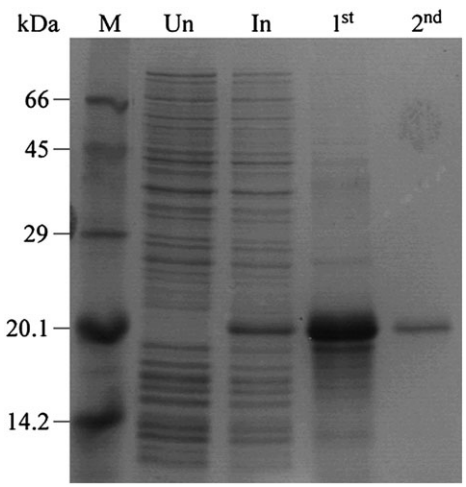

Figure 1 HeleOBP protein expression and purification. Protein from inclusion bodies was purified with two rounds of Ni ion affinity chromatography. M, protein weight marker (BSA, 66 kDa; ovalbumin, 45 kDa; carbonic anhydrase, 29 kDa; trypsin inhibitor, 20.1 kDa; lactalbumin, 14.2 kDa); Un, un-induced bacterial cells; In, induced bacterial cells with IPTG at 0.5 mM final concentration; 1st, first purification round; 2nd, protein with second purification round, delipidation and 2 µM concentration for fluorescence binding assays.

© 2016 The Entomological Society of Japan

vector was added to the *N*-terminal of the OBP. Although the His-tag part could represent interference for binding, its expression in the pNIC28–Bsa4 vector along with the associated tobacco etch virus (TEV) cleavage site make the removal of the His-tag experimentally costly and difficult at large scale. Furthermore, we considered the fact that in some insect OBPs the *C*-terminal section, instead of the *N*-terminal, has an important role for binding. Therefore, it was thought that the His-tagged OBP would still represent a functional recombinant protein from which to obtain binding data.

Fluorescence binding assays

To determine the binding affinity of recombinant HeleOBP (rHeleOBP) to several volatiles, we first measured the affinity of the fluorescent probe 1-NPN to rHeleOBP. The results showed a good binding between 1-NPN and rHeleOBP (Fig. 2) with a binding constant (K_d) of 9.52 μM. Once corroborated with the binding of HeleOBP/1-NPN, competitive binding was performed using host-plant *N. obliqua* volatiles identified by our laboratory and volatiles reported by Quiroz *et al.* (1999). Thus, no strong binding was found for most volatiles tested (Table 1). However, some of them (e.g. benzaldehyde, cinnamaldehyde and host-plant volatiles) could displace 1-NPN from the binding site of HeleOBP, but high concentrations (>40 μM) were needed. The low binding affinity to the volatiles tested shows that HeleOBP is either not specific or its true ligand(s) was (were) not found and tested in this study.

Putative sex pheromones for *H. elegans* such as 1,4-hydroquinone and 1,4-benzoquinone reported by Quiroz *et al.* (2007) were also used as competitors for the binding study. (*E*)-2-nonen-1-ol, a sex pheromone reported for several *Anomala* beetles, was also included. Moreover, we identified a compound released from females of *H. elegans*, acetoin. Results showed no strong binding between HeleOBP and the putative sex pheromones even though HeleOBP could bind with low affinity to 1,4-hydroquinone (K_i = 53.0 μM) and (*E*)-2-nonen-1-ol (K_i = 47.6 μM). Considering that host-plant volatiles identified here were not strong competitors to displace 1-NPN, we selected other volatiles with a significant reported role for the subfamily Rutelinae to which *H. elegans* belongs. Thus, both kairomones and attractants from Pherobase (http://www.pherobase.com/) were selected. From the scarab beetle-related compounds, α-ionone, β-ionone and 2-phenyl acetaldehyde showed good binding to HoblOBPs. However, β-ionone was the strongest in terms of binding. The binding affinities of these compounds and other compounds tested in this study are shown in Figure S2. The results indicate that aromatic compounds such as geraniol, eugenol, 2-phenyl ethanol, 2-phenylethyl propionate, 2-phenyl acetonitrile and cinnamyl alcohol had an appreciable binding affinity to HeleOBP at relatively high concentrations (K_i = 46.2, 44.9, 42.2, 44.9, 51.7 and 39.4 μM, respectively). However, 2-phenyl acetaldehyde had the lowest K_i (16.3 μM) and the highest affinity to HeleOBP among the aromatics ligands. Surprisingly, both α-ionone and β-ionone were bound strongly to HeleOBP with K_i values of 21.4 μM for α-ionone and 6.9 μM for β-ionone (Fig. 3). Moreover, the appreciable difference in the binding affinity to HeleOBP between these two terpenoid isomers suggests that HeleOBP can bind selectively to terpenoids and discriminate between two highly similar ligands.

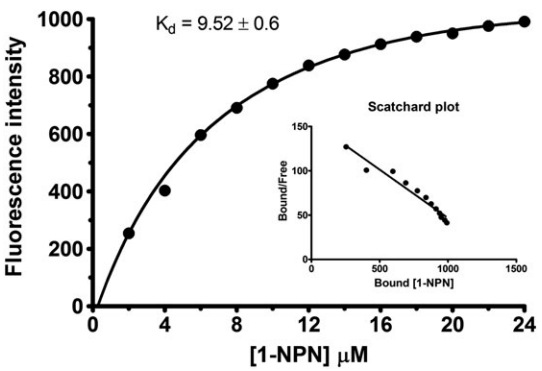

Figure 2 Binding curve of 1-NPN and Scatchard plot for the OBP of *H. elegans*. A 2 μM solution of HeleOBP in Tris buffer was titrated with 1 mM solution of 1-NPN in methanol to final concentrations of 2–24 μM. The dissociation constant (K_d) (from the average of three replicates) was determined using Prism software.

Protein structure prediction and molecular docking

There are no OBP structures determined for any beetles yet. However, experimentally determined three-dimensional (3D) structures of insect OBPs, including for moths and mosquitoes, are available in Protein Data Bank (PDB) (http://www.rcsb.org/pdb/home/home.do). In an attempt to understand the interaction between HeleOBP and the chemicals tested in this study, we predicted the 3D structure of HeleOBP by homology modeling, which is characterized as the best method currently used for protein structure prediction (Bordoli & Schwede 2012; Ravna & Sylte 2012). Moreover, we used multiple templates to improve the quality of models (Larsson *et al.* 2008). The OBPs from mosquito *Anopheles gambiae* (AgamOBP1) (PDB, 2ERB) and *Culex quinquefasciatus* (CquiOBP1) (PDB, 2L2C and 3OGN) were used as templates to build the structural model of HeleOBP. There is 33–35% sequence identity between HeleOBP and the

© 2016 The Entomological Society of Japan

Table 1 Binding affinities of HeleOBP1 to host-plant volatiles and compounds with reported significance for scarab beetles

Ligand	K_i (μM)	IC_{50} (μM)	Molecular formula	HPV	PP	K	A
Terpenes							
β-Caryophyllene	–	–	$C_{15}H_{24}$	♦			
α-Gurjunene	–	–	$C_{15}H_{24}$	♦			
(+)-Aromadendrene	–	–	$C_{15}H_{24}$	♦			
β-Ocimene	–	–	$C_{10}H_{16}$	♦			
α-Pinene	–	–	$C_{10}H_{16}$				●
Geraniol	46.2	34	$C_{10}H_{18}O$				●
α-Ionone	21.4	16	$C_{13}H_{20}O$				●
β-Ionone	6.9	5	$C_{13}H_{20}O$				●
β-Myrcene	–	–	$C_{10}H_{16}$	♦			
(±)-Linalool	50.3	37	$C_{10}H_{18}O$	♦			
Alkanes							
Dodecane	–	–	$C_{12}H_{26}$	♦			
Tetradecane	–	–	$C_{14}H_{26}$	♦			
Alcohols							
(*E*)-2-nonen-1-ol	47.6	35	$C_9H_{16}O$		●		
Heptan-2-ol	–	–	$C_7H_{16}O$				●
Esters							
(*Z*)-3-hexenyl acetate	–	–	$C_8H_{14}O_2$	♦			
Hexyl acetate	53.0	39	$C_8H_{16}O_2$	●			
Aldehydes							
Nonanal	54.4	40	$C_9H_{18}O$	●			
Decanal	49.0	36	$C_{10}H_{20}O$	●			
Ketone							
Acetoin	–	–	$C_4H_8O_2$		●		
Aromatics							
Phenol	–	–	C_6H_6O	●			
Benzaldehyde	49.0	36	C_7H_6O	●			
1,4-Benzoquinone	–	–	$C_6H_4O_2$		●		
1,4-Hydroquinone	53.0	39	$C_6H_6O_2$		●		
Eugenol	44.9	33	$C_{10}H_{12}O_2$				●
2-Phenyl acetaldehyde	16.3	12	C_8H_8O			●	
2-Phenyl ethanol	42.2	31	$C_8H_{10}O$			●	
2-Phenylethyl propionate	44.9	33	$C_{11}H_{14}O_2$				●
2-Phenyl acetonitrile	51.7	38	C_8H_7N			●	
Cinnamyl alcohol	39.4	29	$C_9H_{10}O$				●

K_i, dissociation constant; IC_{50}, concentration of ligand halving the initial fluorescence intensity; –, data not available; ●, role of the ligand for scarab beetles reported in literature (HPV, host plant volatiles; PP, putative pheromone; K, kairomone; A, attractant); ♦, ligands identified from the host-plant of *H. elegans* in this study.

templates, which is considered good enough to obtain accurate models (Schwede *et al.* 2007). The 3D structure of HeleOBP suggests the presence of six α-helices as the main feature of insect OBPs (Pelosi *et al.* 2006) located between amino acids as follows: Glu3-Thr20 (α1), Glu24-Asp32 (α2), Glu40-Met53 (α3), Val64-Ile70 (α4), Asp73-Arg84 (α5) and Pro94-Thr108 (α6). Likewise, a multiple sequence alignment between the templates and HeleOBP indicates the presence of six conserved Cys residues (Fig. S3). Subsequently, the 3D model of the protein showed three connected disulfide bridges: Cys16–Cys48, Cys44–Cys95 and Cys86–Cys104. The presence of three disulfide bridges allow us to classify HeleOBP as a classic OBP as has been suggested by several authors (Zhou 2010; Fan *et al.* 2011). The modeled structure of HeleOBP was then used to calculate *in silico* its binding affinity to a wide range of chemicals by molecular docking based on free binding energy and a size-independent score called fit quality (FQ). It is worth mentioning that there was a strong dependence between the free binding energy, commonly calculated by docking software such as Autodock, and ligand molecular size (Fig. S4) as reported in other studies (Reynolds *et al.* 2007). This finding allowed us to use FQ for the affinity

© 2016 The Entomological Society of Japan

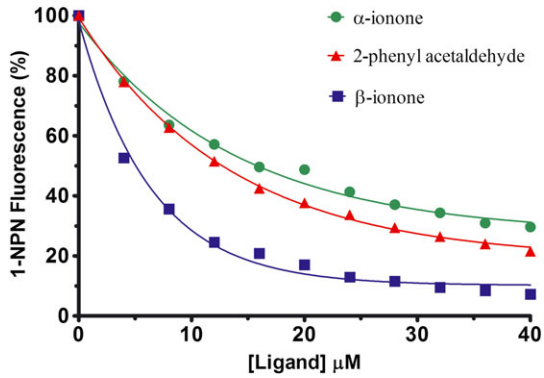

Figure 3 Competitive binding of HeleOBP to α-ionone (21.4 μM), β-ionone (6.9 μM) and 2-phenyl acetaldehyde (16.3 μM). A 2 μM solution of the protein plus 1-NPN was titrated with 1 mM solutions of each ligand in methanol to final concentrations of 4–40 μM.

calculation and compare the score with those obtained by the fluorescent binding assay. The molecular docking suggests that HeleOBP could provide a good accommodation for acetoin, phenol, benzaldehyde, sesquiterpenes, α-ionone and β-ionone in terms of FQ. However, free binding energy still suggests α- and β-ionone as highly stable binders to HeleOBP. Thus, the *in silico* binding assays suggested the participation of four main residues, His102, Tyr105, Tyr113 and Met114, in the stabilization of the complex of HeleOBP with the strong binding ligands (α-ionone, β-ionone and 2-phenyl acetaldehyde) (Fig. 4). Acetoin showed a high FQ (>1.0) and the highest K_i (3.52 mM), suggesting a good fit but bad protein–ligand stability. On the other hand, the binding of 2-phenyl acetaldehyde showed FQ = 0.73 and an experimental K_i = 16.3 μM, suggesting a good fit for the ligand.

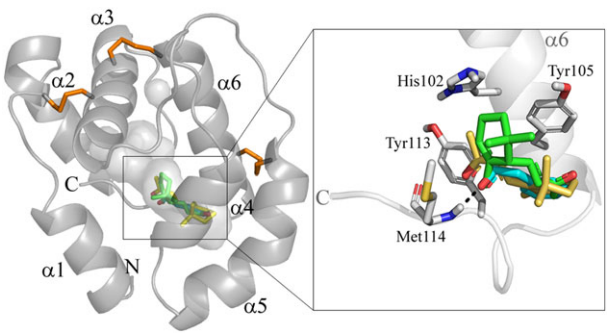

Figure 4 The homology model of HeleOBP with α-helices displayed as grey ribbons (α1–α6) in complex with the strongest ligands obtained from experimental binding assays. *N*- and *C*-terminals are indicated as *N* and *C*, respectively. Disulfide bonds are highlighted as orange sticks. Square indicates the magnified section as well as the docked conformations of α-ionone (green sticks), β-ionone (yellow sticks) and 2-phenyl acetaldehyde (light blue sticks). Hydrogen bond is indicated as dashed lines.

Table 2 Binding affinities of HeleOBP1 to the strongest ligands suggested by *in silico* and *in vitro* binding assays

Ligand	$K_{i(exp)}$ (μM)	Binding energy (kcal/mol)	FQ
α-Ionone	21.4	–6.88	0.81
β-Ionone	6.9	–6.99	0.82
2-Phenyl acetaldehyde	16.3	–4.78	0.73

FQ, fit quality; $K_{i(exp)}$, experimentally determined dissociation constant.

Molecular docking was successful in rendering the difference between β-ionone (FQ = 0.82; –6.99 kcal/mol) and 2-phenyl acetaldehyde (FQ = 0.73; –4.78 kcal/mol) (Table 2). Similarly, but less noticeably, the *in silico* approach suggested α- and β-ionone as strong ligands in terms of both free binding energy and FQ. Here, four main residues are predicted to participate in HeleOBP–ligand complexes supporting, particularly, good binding of β-ionone.

Electroantennographic responses

The three strongest ligands (α-ionone, β-ionone and 2-phenyl acetaldehyde) in terms of binding to HeleOBP were selected for EAG recordings. The three ligands elicited EAG responses in antennae of both males and females of *H. elegans* (Fig. 5). However, no dose-dependent responses were obtained for most of the tested antennae. Despite this, from 10 to 1000 ppm males responded with higher amplitudes to 2-phenyl acetaldehyde, showing a slight dose-dependent response (Fig. 5C). On the other hand, a significant difference between 0.1 and 1.0 ppm of β-ionone was obtained for females (Fig. 5A). The same result was obtained for β-ionone at 1000 ppm compared with 1.0 ppm in females. On the other hand, EAG responses for male antennae indicate significant difference between doses 0.1 and 1.0 ppm, which is similar to the EAG responses of females. Similarly, statistical analyses suggest that α-ionone does not elicit any dose-dependent response in either males or females (Fig. 5B). The two terpenoids elicited stronger responses in males, with >0.75 and 1.00 mV from 0.1 ppm for α-ionone and from 1.0 ppm for β-ionone. Although 2-phenyl acetaldehyde showed an increasing EAG response in males, <0.25 mV amplitude was obtained at lower doses (i.e. 0.1 and 1.0 ppm). It is worth mentioning that the ranges of amplitudes obtained for α-ionone in females and males throughout the doses were similar, and no significant difference was found. However, a rough comparison of dose between α- and β-ionone in females and males suggests that antennae were more sensitive for α-ionone at 0.1 ppm considering their high amplitudes.

© 2016 The Entomological Society of Japan

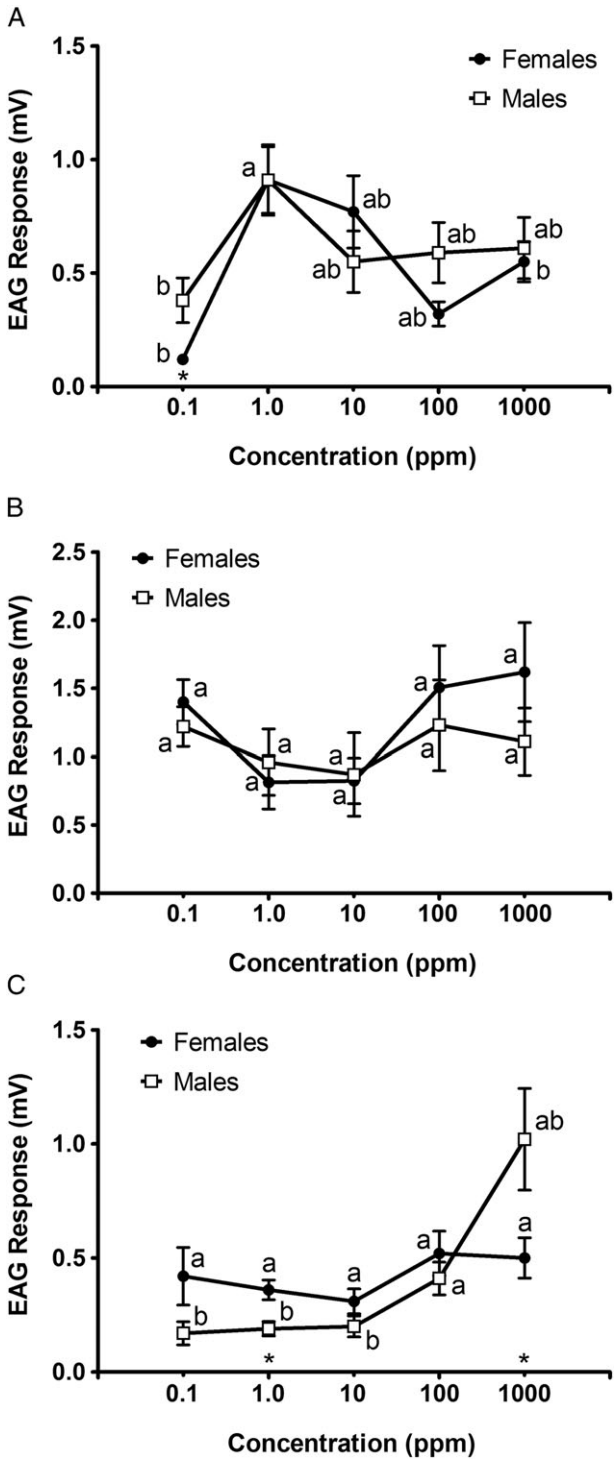

Figure 5 Comparison of EAG responses between males and females for each dose, and doses for each sex. (A) β-ionone; (B) α-ionone; (C) 2-phenyl acetaldehyde. *, significant difference between sex for the same dose. Different letters indicate significant difference between doses for the same sex.

Analyses between sexes showed no difference in EAG response for almost all the stimulus doses (Fig. 5). However, females responded significantly with higher amplitude to 2-phenyl acetaldehyde at 1.0 ppm than males. Likewise, a significant difference was obtained at 1000 ppm for the same chemical, where males were more sensitive. An outstanding response for β-ionone at 0.1 ppm was obtained from males, as males were more electrophysiologically sensitive than females. It is worth mentioning that this terpenoid has been selected as a strong OBP binder, with K_i = 6.9 μM according to our previous results.

DISCUSSION

We have identified a full-length odorant-binding protein (OBP) from antennae of both males and females of *H. elegans*. This protein has been temporarily considered as an OBP because of its presence in both sexes and lack of binding information. Thus, in order to characterize the binding properties of HeleOBP and find putative semiochemicals, we have used several compounds from the main host-plant, *N. obliqua* (Giganti & Dapoto 1990; Artigas 1994; Quiroz *et al.* 1999; Klein & Waterhouse 2000; Lanfranco *et al.* 2001), putative sex pheromones and semiochemicals reported in the literature for scarab beetles, specifically for the subfamily Rutelinae. All these compounds were tested using both fluorescence and *in silico* binding assays, whose results led the application of EAG.

Some putative sex pheromones and a potential source of sexual kairomones were tested here. However, the antennae-identified protein, HeleOBP, showed highly selective binding to compounds reported for other scarab beetles: α-ionone, β-ionone and 2-phenyl acetaldehyde. Despite their strong binding to HeleOBP, the physiological role of these compounds in *H. elegans* is unclear. Deng *et al.* (2012) reported a strong binding of β-ionone to HoblOBP1 and HoblOBP2 with K_i = 6.35 and 5.36 μM, respectively. Moreover, β-ionone has been identified as highly attractive for both males and females of the scarab beetle *Anomala transvaalensis* (Donaldson *et al.* 1990). On the other hand, 2-phenyl acetaldehyde has been reported as a kairomone to which the scarab beetle *A. octiescostata* is attracted. This compound has been highlighted as part of an active mixture from dandelion *Taraxacum officinale*, where volatiles such as (*Z*)-3-hexenyl acetate, benzaldehyde, 2-phenyl acetaldehyde and phenyl acetonitrile participate (Leal *et al.* 1994).

Although α-ionone, β-ionone and 2-phenyl acetaldehyde do not show the strongest binding affinity found for insect OBPs, in this study they are considered the strongest

© 2016 The Entomological Society of Japan

ligands supported not only by fluorescence binding assays but also by molecular docking. Considering that a 3D model of HeleOBP was constructed, the identification of its binding site could represent a challenging task. However, the presence of ligands already bound to the templates (e.g. AgamOBP1–PEG complex and CquiOBP1–MOP complex) helped identify a potential binding site in HeleOBP. Likewise, the consistency between the modeled binding site in HeleOBP and the prediction by the CASTp server provided us the area where molecular docking could be applied. Thus, this last *in silico* method suggested that α-ionone, β-ionone and 2-phenyl acetaldehyde seem to interact with His102, Tyr105 and Tyr113. His102 and Tyr113 are well-conserved residues from part of the binding site of the templates AgamOBP1 and CquiOBP1 (Fig. S5). It is likely that π–π interactions have an important role because of either aromatic characteristics or unsaturations, which can participate when these residues are involved in ligand binding. For example, it has been proposed that this type of interaction could be established when Tyr111 in the binding site of HoblOBP1 interacts with cinnamaldehyde and β-ionone (Zhuang *et al.* 2014). Tyr113 in HeleOBP could play a similar role for β-ionone binding since the residue is well aligned to Tyr111. On the other hand, α- and β-ionone have highly similar structures, although different binding modes were obtained (Fig. 4). One large conformational cluster was obtained from the complexes HeleOBP–ionones in Autodock, where limited movement of α- and β-ionone (i.e. two rotatable bonds) was shown. It is probable that these docking characteristics resulted in one stable binding mode for both ionones but opposite from each other. A closest view of the binding modes of these terpenoids would involve the dynamics of the complexes, where the movement of ligands into the binding site and a likely formation of hydrogen bonds could explain the above finding. For instance, a recent study on the moth *Loxostege sticticalis* has reported the key role of Thr15 and Trp43 in the binding site of *L. sticticalis* OBP1 (LstiOBP1). Multiple hydrogen bonds seemed to be interrupted when both Thr15 and Trp43 were mutated to Ala. A decrease of the binding affinity of ligands such as heptanol, (*E*)-11-tetradecenyl acetate, cinnamic aldehyde and (*E*)-2-hexenal to $>40\,\mu M$ of K_d was obtained (Yin *et al.* 2015). For 2-phenyl acetaldehyde, it seems that the carbonyl group can form a hydrogen bond with the amino moiety of Met114. This residue could participate actively in forming the binding site of HeleOBP (Fig. 4). The modeled structure of HeleOBP showed the *C*-terminal section forms a lid on the binding site, which makes Met114 free to establish interactions. Therefore, the *C*-terminal section might play a key role for ligand binding as it has been widely proposed for moth OBPs such as *Bombyx mori* PBP1 (BmorPBP1) (Horst *et al.* 2001; Lautenschlager *et al.* 2005; Leal 2005).

The binding of HeleOBP supported by fluorescence binding assays and molecular docking indicated β-ionone as a strong OBP-binder as it has been found for other scarab beetles such as *H. oblita*. Although β-ionone was active for females, lower sensitivity in females than in males was exhibited. Lower EAG responses have also been found for β-ionone in females compared with other chemicals such as cinnamaldehyde, myrcene, methyl salicylate and 2,4-di-tert-butylphenol (Deng *et al.* 2012). Thus, it is possible that a number of β-ionone-tuned ORs are part of the male antennae, explaining the sensitivity obtained at low concentrations in males. Despite the results obtained, it is still unclear where this compound is present in the context of *H. elegans*. This terpenoid might play a key role at some stage of the life cycle of *H. elegans*, considering that β-ionone has been reported in red clover *T. pratense* (Figueiredo *et al.* 2007). However, contrary to the sensitivity showed by males, gravid females have been reported flying to crops such as *T. pratense* (Artigas 1994). This last behavior could be explained because females are more sensitive to several factors of host-plants, such as non-volatile secondary metabolites, surface structure, tissue toughness and water content, than only to volatiles as semiochemicals. Thus, females could ensure a host-plant with high nutritive value for themselves and their offspring. On the other hand, it has been proposed that because of the priority of mate finding, males are more sensitive to volatiles from either host-plants or damaged plants, where they can find potential mates (Fernandez & Hilker 2007). Although our results indicate β-ionone as a potential bioactive volatile, more evidence is necessary to establish it as semiochemical for *H. elegans*.

Hitherto, only one significant attractive blend for *H. elegans* (1,4-benzoquinone and essential oil from *N. obliqua*) has been reported. Likewise, neither pheromone nor kairomone has been identified for this scarab beetle. Although the binding characteristics of HeleOBP examined here suggest that the protein is not tuned to host-plant volatiles, binding mechanisms could play a crucial role for active ligands at OR level, as has recently been proposed by Murphy *et al.* (2013). Likewise, it is probable that other OBPs could be actively participating in host-plant volatile transport. Further experiments are necessary to determine other OBPs present in *H. elegans* as well as the role of the semiochemical-candidate compounds found in this work. Finally, our results represent the first step of a semiochemical screening in *H. elegans* starting from molecular approaches.

© 2016 The Entomological Society of Japan

ACKNOWLEDGMENTS

This research was partially supported by the supercomputing infrastructure of the NLHPC (ECM-02) at Centro de Modelación y Computación Científica, Universidad de La Frontera, CMCC-UFRO, Chile. This work was supported by CONICYT (21110933), DIUFRO DI 10-0018 and Rothamsted Research, which receives grant-aided support from the Biotechnology and Biological Sciences Research Council (BBSRC) of the United Kingdom. We thank Dr Ricardo Ceballos from Instituto de Investigaciones Agropecuarias (INIA), Quilamapu, Laboratorio de Ecología Química, Chillán, Chile, for his valuable help during the development and analysis of electroantennographic recordings. Thanks to Professor Nick Keep, University of London, UK, for the kind gift of expression vector pNIC28.

REFERENCES

Alzari PM, Berglund H, Berrow NS *et al.* (2006) Implementation of semi-automated cloning and prokaryotic expression screening: the impact of SPINE. *Acta Crystallographica Section D: Biological Crystallography* **62**, 1103–1113.

Artigas J (1994) *Hylamorpha elegans* (Burmeister). Pololo San Juan verde (San Juan green beetle). In: Artigas J (ed.) *Entomología Económica. Insectos de Interés Agrícola, Forestal, Médico y Veterinario*, pp 344–346. Universidad de Concepción, Editorial Universidad de Concepción, Concepción, Chile.

Aslanidis C, de Jong PJ (1990) Ligation-independent cloning of PCR products (LIC-PCR). *Nucleic Acids Research* **18**, 6069–6074.

Bembenek SD, Tounge BA, Reynolds CH (2009) Ligand efficiency and fragment-based drug discovery. *Drug Discovery Today* **14**, 278–283.

Bordoli L, Schwede T (2012) Automated protein structure modeling with SWISS-MODEL Workspace and the protein model portal. In: Orry AJW, Abagyan R, Molsoft LLC (eds) *Homology Modeling: Methods and Protocols*, pp 107–136. Humana Press, San Diego, CA.

Deng S, Yin J, Zhong T, Cao Y, Li K (2012) Function and immunocytochemical localization of two novel odorant-binding proteins in olfactory sensilla of the scarab beetle *Holotrichia oblita* Faldermann (Coleoptera: Scarabaeidae). *Chemical Senses* **37**, 141–150.

Donaldson JMI, McGovern TP, Ladd JTL (1990) Floral attractants for Cetoniinae and Rutelinae (Coleoptera: Scarabaeidae). *Journal of Economic Entomology* **83**, 1298–1305.

Dundas J, Ouyang Z, Tseng J, Binkowski A, Turpaz Y, Liang J (2006) CASTp: computed atlas of surface topography of proteins with structural and topographical mapping of functionally annotated residues. *Nucleic Acids Research* **34**, W116–W118.

Fan J, Francis F, Liu Y, Chen JL, Cheng DF (2011) An overview of odorant-binding protein functions in insect peripheral olfactory reception. *Genetics and Molecular Research* **10**, 3056–3069.

Fernandez P, Hilker M (2007) Host plant location by Chrysomelidae. *Basic and Applied Ecology* **8**, 97–116.

Figueiredo R, Rodrigues AI, do Céu Costa M (2007) Volatile composition of red clover (*Trifolium pratense* L.) forages in Portugal: The influence of ripening stage and ensilage. *Food Chemistry* **104**, 1445–1453.

Giganti H, Dapoto G (1990) Coleópteros de los bosques nativos del Departamento Aluminé (Neuquén-Argentina). *Bosque* **11**, 37–44.

Gong Y, Pace TCS, Castillo C, Bohne C, O'Neill M, Plettner E (2009) Ligand-interaction kinetics of the pheromone-binding protein from the gypsy moth, *L. dispar*: Insights into the mechanism of binding and release. *Chemistry & Biology* **16**, 162–172.

Guo L, Li GQ (2009) Olfactory perception of oviposition-deterring fatty acids and their methyl esters by the Asian corn borer, *Ostrinia furnacalis*. *Journal of Insect Science* **9**, Article ID 67. DOI:10.1673/031.009.6701

Horst R, Damberger F, Luginbühl P *et al.* (2001) NMR structure reveals intramolecular regulation mechanism for pheromone binding and release. *Proceedings of the National Academy of Sciences* **98**, 14 374–14 379.

Ishida Y, Leal WS (2002) Cloning of putative odorant-degrading enzyme and integumental esterase cDNAs from the wild silkmoth, *Antheraea polyphemus*. *Insect Biochemistry and Molecular Biology* **32**, 1775–1780.

Ishida Y, Chiang V, Haverty M, Leal WS (2002) Odorant-binding protein from a primitive termite. *Journal of Chemical Ecology* **28**, 1887–1893.

Ju Q, Qu M-J, Wang Y *et al.* (2012) Molecular and biochemical characterization of two odorant-binding proteins from dark black chafer, *Holotrichia parallela*. *Genome* **55**, 537–546.

Kaissling K-E (2013) Kinetics of olfactory responses might largely depend on the odorant-receptor interaction and the odorant deactivation postulated for flux detectors. *Journal of Comparative Physiology A* **199**, 879–896.

Klein C, Waterhouse DF (2000) *The Distribution and Importance of Arthropods Associated with Agriculture and Forestry in Chile*. ACIAR Monograph N°68, Canberra.

Kowcun A, Honson N, Plettner E (2001) Olfaction in the gypsy moth, *Lymantria dispar*: Effect of pH, ionic strength, and reductants on pheromone transport by pheromone-binding proteins. *Journal of Biological Chemistry* **276**, 44770–44776.

Lagarde A, Spinelli S, Tegoni M *et al.* (2011) The crystal structure of odorant binding protein 7 from *Anopheles gambiae* exhibits an outstanding adaptability of its binding site. *Journal of Molecular Biology* **414**, 401–412.

Lanfranco D, Rojas E, Ríos R, Ruíz C (2001) Insect defoliators of *Nothofagus obliqua* (Roble) in South Chile: Two years monitoring species and their damage. In: Liebhold AM, McManus ML, Otvos IS, Fosbroke SLC (eds) *Proceedings: Integrated Management and Dynamics of Forest Defoliating Insects*, pp 91–103. U.S. Department of Agriculture,

© 2016 The Entomological Society of Japan

Forest Service, Northeastern Research Station, Newtown Square, PA.

Larsson P, Wallner B, Lindahl E, Elofsson A (2008) Using multiple templates to improve quality of homology models in automated homology modeling. *Protein Science* **17**, 990–1002.

Laskowski RA, MacArthur MW, Moss DS, Thornton JM (1993) PROCHECK: a program to check the stereochemical quality of protein structures. *Journal of Applied Crystallography* **26**, 283–291.

Laughlin JD, Ha TS, Jones DNM, Smith P (2008) Activation of pheromone-sensitive neurons is mediated by conformational activation of pheromone-binding protein. *Cell* **133**, 1255–1265.

Lautenschlager C, Leal WS, Clardy J (2005) Coil-to-helix transition and ligand release of *Bombyx mori* pheromone-binding protein. *Biochemical and Biophysical Research Communications* **335**, 1044–1050.

Leal WS (1998) Chemical ecology of phytophagous scarab beetles. *Annual Review of Entomology* **43**, 39–61.

Leal WS (2005) Pheromone reception. *Topics in Current Chemistry* **240**, 1–36.

Leal WS, Ono M, Hasegawa M, Sawada M (1994) Kairomone from dandelion, *Taraxacum officinale*, attractant for scarab beetle *Anomala octiescostata*. *Journal of Chemical Ecology* **20**, 1697–1704.

Morris GM, Goodsell DS, Halliday RS *et al.* (1998) Automated docking using a lamarckian genetic algorithm and an empirical binding free energy function. *Journal of Computational Chemistry* **19**, 1639–1662.

Morris GM, Huey R, Lindstrom W *et al.* (2009) Autodock 4 and AutoDockTools4: automated docking with selective receptor flexibility. *Journal of Computational Chemistry* **16**, 2785–2791.

Murphy EJ, Booth JC, Davrazou F, Port AM, Jones DNM (2013) Interactions of *Anopheles gambiae* odorant-binding proteins with a human-derived repellent. *Journal of Biological Chemistry* **288**, 4475–4485.

Mutis A, Palma R, Parra L *et al.* (2014) Morphology and distribution of sensilla on the antennae of *Hylamorpha elegans* Burmeister (Coleoptera: Scarabaeidae). *Neotropical Entomology* **43**, 260–265.

Pelosi P, Calvello M, Ban L (2006) Diversity of odorant-binding proteins and chemosensory proteins in insects. *Chemical Senses* **30**, 291–292.

Plettner E, Lazar J, Prestwich EG, Prestwich GD (2000) Discrimination of pheromone enantiomers by two pheromone binding proteins from the gypsy moth *Lymantria dispar*. *Biochemistry* **39**, 8953–8962.

Quiroz A, Fuentes-Contreras E, Ramírez CC, Russell GB, Niemeyer HM (1999) Host-plant chemicals and distribution of *Neuquenaphis* on *Nothofagus*. *Journal of Chemical Ecology* **25**, 1043–1054.

Quiroz A, Palma R, Etcheverría P, Navarro V, Rebolledo R (2007) Males of *Hylamorpha elegans* Burmeister (Coleoptera: Scarabaeidae) are attracted to odors released from conspecific females. *Environmental Entomology* **36**, 272–280.

Ravna AW, Sylte I (2012) Homology modeling of transporter proteins (carriers and ion channels). In: Orry AJW, Abagyan R, Molsoft LLC (eds) *Homology Modeling: Methods and Protocols*, pp 281–299. Humana Press, San Diego, CA.

Reinecke A, Ruther J, Tolasch T, Francke W, Hilker M (2002) Alcoholism in cockchafers: orientation of male *Melolontha melolontha* towards green leaf alcohols. *Naturwissenschaften* **89**, 265–269.

Reinecke A, Ruther J, Hilker M (2005) Electrophysiological and behavioural responses of *Melolontha melolontha* to saturated and unsaturated aliphatic alcohols. *Entomologia Experimentalis et Applicata* **115**, 33–40.

Reynolds CH, Bembenek SD, Tounge BA (2007) The role of molecular size in ligand efficiency. *Bioorganic & Medicinal Chemistry* **17**, 4258–4261.

Ruther J, Reinecke A, Thiemann K, Tolasch T, Francke W, Hilker M (2000) Mate finding in the forest cockchafer, *Melolontha hippocastani*, mediated by volatiles from plants and females. *Physiological Entomology* **25**, 172–179.

Schwede T, Sali A, Eswar N, Peitsch MC (2007) Protein structure modeling. In: Schwede T, Peitsch MC (eds) *Computational Structural Biology – Methods and Applications, World Scientific*, pp 3–35. World Scientific Publishing Company, Danvers, MA.

Siciliano P, He XL, Woodcock C *et al.* (2014) Identification of pheromone components and their binding affinity to the odorant binding protein CcapOBP83a-2 of the Mediterranean fruit fly, *Ceratitis capitata*. *Insect Biochemistry and Molecular Biology* **48**, 51–62.

Sokkar P, Mohandass S, Ramachandran M (2011) Multiple templates-based homology modeling enhances structure quality of AT1 receptor: validation by molecular dynamics and antagonist docking. *Journal of Molecular Modelling* **17**, 1565–1577.

Vogt RG, Riddiford LM (1981) Pheromone binding and inactivation by moth antennae. *Nature* **293**, 161–163.

Vuts J, Imrei Z, Birkett MA, Pickett JA, Woodcock CM, Tóth M (2014) Semiochemistry of the Scarabaeoid. *Journal of Chemical Ecology* **40**, 190–210.

Wang B, Li K, Yin J, Cao Y (2013) Potential cooperations between odorant-binding proteins of the scarab beetle *Holotrichia oblita* Faldermann (Coleoptera: Scarabaeidae). *PLoS ONE* **8**, Article ID, e84795. DOI:10.1371/journal.pone.0084795

Wojtasek H, Picimbon J, Leal W (1999) Identification and cloning of odorant binding proteins from the scarab beetle *Phyllopertha diversa*. *Biochemical and Biophysical Research Communications* **263**, 832–837.

Yin J, Zhuang X, Wang Q *et al.* (2015) Three amino acid residues of an odorant-binding protein are involved in binding odours in *Loxostege sticticalis* L. *Insect Molecular Biology* **24**, 528–538.

Zhou J-J (2010) Odorant-binding proteins in insects. In: Litwack G (ed.) *Vitamins and Hormones*, pp 241–272. Academic Press, Burlington, MA.

Zhuang X, Wang Q, Wang B *et al.* (2014) Prediction of the key binding site of odorant-binding protein of *Holotrichia oblita* Faldermann (Coleoptera: Scarabaeidae). *Insect Molecular Biology* **23**, 381–390.

© 2016 The Entomological Society of Japan

SUPPORTING INFORMATION

Additional Supporting Information may be found in the online version of this article at the publisher's web-site:

Table S1 Oligonucleotide primers designed for cDNA cloning and sub-cloning of the OBP in *H. elegans*.
Figure S1 Phylogenetic tree with scarab OBPs available from NCBI (http://www.ncbi.nlm.nih.gov/).
Figure S2 Competitive binding of HeleOBP to selected odorants.
Figure S3 Multiple sequence alignment among HeleOBP, AgamOBP1 (PDB code: 2ERB) and CquiOBP1 (PDB code: 2L2C and 3OGN).
Figure S4 Correlation between free binding energy and molecular size as heavy atoms (non-hydrogen) from molecular docking.
Figure S5 Super-imposed 3D structures of HeleOBP (green), AgamOBP1 (PDB code: 2ERB) (light blue) and CquiOBP1 (PDB code: 3OGN) (yellow).

Entomological Science (2016) **19**, 188–200
© 2016 The Entomological Society of Japan